

CERN-TH/99-306
MC-TH-99-14
October 1999

Predicting $F_2^{D(3)}$ from the dipole cross-section

J. R. Forshaw*, G. R. Kerley and G. Shaw^a

^aTheoretical Physics Group, Department of Physics and Astronomy,
The University of Manchester, M13 9PL, UK

We employ a parameterisation of the proton dipole cross section previously extracted from electroproduction and photoproduction data to predict the diffractive structure function $F_2^{D(3)}(Q^2, \beta, x_P)$. Comparison with HERA H1 data yields good agreement.

1. Introduction

The proton dipole cross section σ_d is a universal quantity in singly dissociative diffractive γp processes. [1,2] It is simply the total cross section for scattering a $q\bar{q}$ pair of a given size and energy in the photonic fluctuation off the proton target. We make use of a parameterisation used to extract σ_d from a fit to electroproduction and photoproduction γp total cross-section data [3] to predict the diffractive structure function $F_2^{D(3)}(Q^2, \beta, x_P)$.

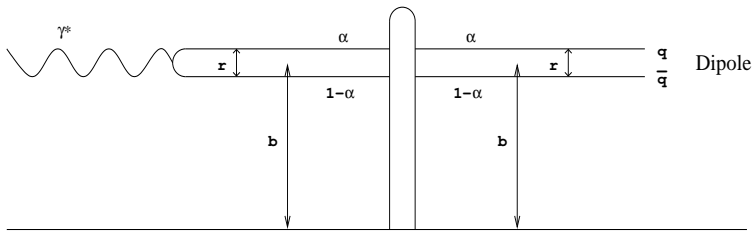


Figure 1. The dipole fluctuation of the incoming photon.

2. Functional forms

The dipole cross-section is in general a function of three variables (Figure 1): $s = W^2$, the CMS energy squared of the photon proton system; r , the transverse separation averaged over all orientations of the $q\bar{q}$ pair; and α , the fraction of the incoming photon light cone energy possessed by one member of the $q\bar{q}$ pair. We assumed a form with two

*Theory Division, CERN, 1211 Geneva 23, Switzerland.

terms, each with a Regge type s dependence and no dependence on α . Specifically, we assumed

$$\sigma_d(s, r) = a_0^S \left(1 - \frac{1}{1 + (a_1^S r + a_2^S r^2)^2} \right) (r^2 s)^{\lambda_S} + (a_1^H r + a_2^H r^2 + a_3^H r^3)^2 \exp(-\nu_H^2 r) (r^2 s)^{\lambda_H}. \quad (1)$$

The dipole cross section is related to the photon proton cross section via

$$\sigma_{\gamma^*, p}^{L, T} = \int d\alpha d^2 r |\psi_\gamma^{L, T}(\alpha, r)|^2 \sigma_d(s, r, \alpha) \quad (2)$$

where $\psi_\gamma^{L, T}(\alpha, r)$ are the longitudinal and transverse components of the light cone photon wave function. For the photon wave function itself, we used the tree level QED expression [1,4] modified by a factor $f(r)$ to represent confinement effects:

$$|\psi_L(\alpha, r)|^2 = \frac{6}{\pi^2} \alpha_{em} \sum_{q=1}^3 e_q^2 Q^2 \alpha^2 (1 - \alpha)^2 K_0^2(\epsilon r) \times f(r) \quad (3)$$

$$|\psi_T(\alpha, r)|^2 = \frac{3}{2\pi^2} \alpha_{em} \sum_{q=1}^3 e_q^2 \left\{ [\alpha^2 + (1 - \alpha)^2] \epsilon^2 K_1^2(\epsilon r) + m_f^2 K_0^2(\epsilon r) \right\} \times f(r) \quad (4)$$

and

$$f(r) = \frac{1 + B \exp(-c^2(r - R)^2)}{1 + B \exp(-c^2 R^2)}. \quad (5)$$

Here $\epsilon^2 = \alpha(1 - \alpha)Q^2 + m_f^2$, K_0 and K_1 are modified Bessel functions and the sum is over 3 light quark flavours, with a generic mass of assumed value $m_f^2 = 0.08 \text{ GeV}^2$. The values of the constants B , c^2 , and R were generated by the fit.

3. Calculating $F_2^{D(3)}$

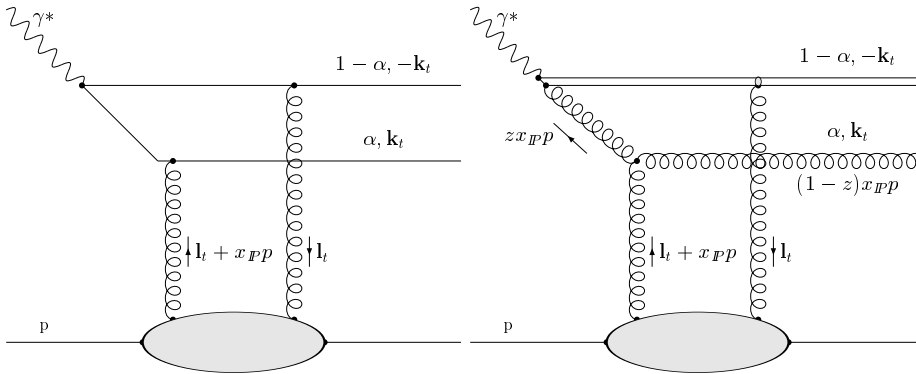


Figure 2. The $q\bar{q}$ and $q\bar{q}g$ contributions to $F_2^{D(3)}$.

To calculate the contribution of the quark antiquark dipole to $F_2^{D(3)}$ we made use of expressions derived from a momentum space treatment [5,6]. Also, we calculated the contribution of the higher $q\bar{q}g$ Fock state using an effective two gluon dipole description from the same source. Typical Feynman diagrams are shown in Figure 2. For compatibility with this approach, we must replace s by \tilde{s} , where $\tilde{s} = Q^2(1/x_P - 1)$. First defining

$$\Phi_{0,1} \equiv \int_0^\infty r dr K_{0,1}(\epsilon r) \sigma_d(r, \tilde{s}) J_{0,1}(kr) \int_0^\infty r dr f(r) K_{0,1}(\epsilon r) \sigma_d(r, \tilde{s}) J_{0,1}(kr), \quad (6)$$

we have for the longitudinal and transverse $q\bar{q}$ components respectively

$$x_P F_{q\bar{q},L}^D(Q^2, \beta, x_P) = \frac{3Q^6}{32\pi^4 \beta b} \cdot \sum_{f=1}^3 e_f^2 \cdot 2 \int_{\alpha_0}^{1/2} d\alpha \alpha^3 (1-\alpha)^3 \Phi_0 \quad (7)$$

$$x_P F_{q\bar{q},T}^D(Q^2, \beta, x_P) = \frac{3Q^4}{128\pi^4 \beta b} \cdot \sum_{f=1}^3 e_f^2 \cdot 2 \int_{\alpha_0}^{1/2} d\alpha \alpha (1-\alpha) \left\{ \epsilon^2 [\alpha^2 + (1-\alpha)^2] \Phi_1 + m^2 \Phi_0 \right\} \quad (8)$$

where the lower limit of the integral over α is given by $\alpha_0 = (1/2) \left(1 - \sqrt{1 - 4m_f^2/M_X^2}\right)$ and b is the slope parameter, which we have taken as 7.2 [7]. For the $q\bar{q}g$ term we have

$$x_P F_{q\bar{q}g}^D(Q^2, \beta, x_P) = \frac{81\beta\alpha_S}{512\pi^5 b} \sum_f e_f^2 \int_\beta^1 \frac{dz}{(1-z)^3} \left[\left(1 - \frac{\beta}{z}\right)^2 + \left(\frac{\beta}{z}\right)^2 \right] \quad (9)$$

$$\times \int_0^{(1-z)Q^2} dk_t^2 \ln \left(\frac{(1-z)Q^2}{k_t^2} \right) \left[\int_0^\infty u du \sigma_d(u/k_t, \tilde{s}) K_2 \left(\sqrt{\frac{z}{1-z}} u \right) J_2(u) \right]^2 \quad (10)$$

with $\alpha_S = 0.2$. (We have inserted a missing factor of 1/2 compared with the expression in [6].) This expression diverges if our parameterisation is used as it stands. However, this is due solely to the mild divergence after σ_d saturates in r of the factor $(r^2 s)^{\lambda_S}$ as $r \rightarrow \infty$. This behaviour at large r is not determined by data and is an artefact of the parameterisation. Hence we have imposed a saturation value for σ_d of its value at $r = 2$ fm for all higher r . Plots of the contributions to $x_P F_2^{D(3)}$ calculated from these expressions are compared with H1 1994 data [8] in Figure 3. Agreement is good, even at low β where the $q\bar{q}g$ term dominates. Comparison with ZEUS 1994 data [9] also gives good agreement overall but with deviations at larger Q^2 values for small and moderate β .

4. Conclusions

We have successfully predicted the diffractive structure function $F_2^{D(3)}$ using a parameterised dipole cross section obtained from electro- and photoproduction data. Unlike the model proposed in [6,10], the parameterisation exhibits effective saturation in r only, with no saturation in the energy variable $s = W^2$. Agreement with data is reasonable, leading to the conclusion that the HERA data do not necessarily indicate such saturation at present energies.

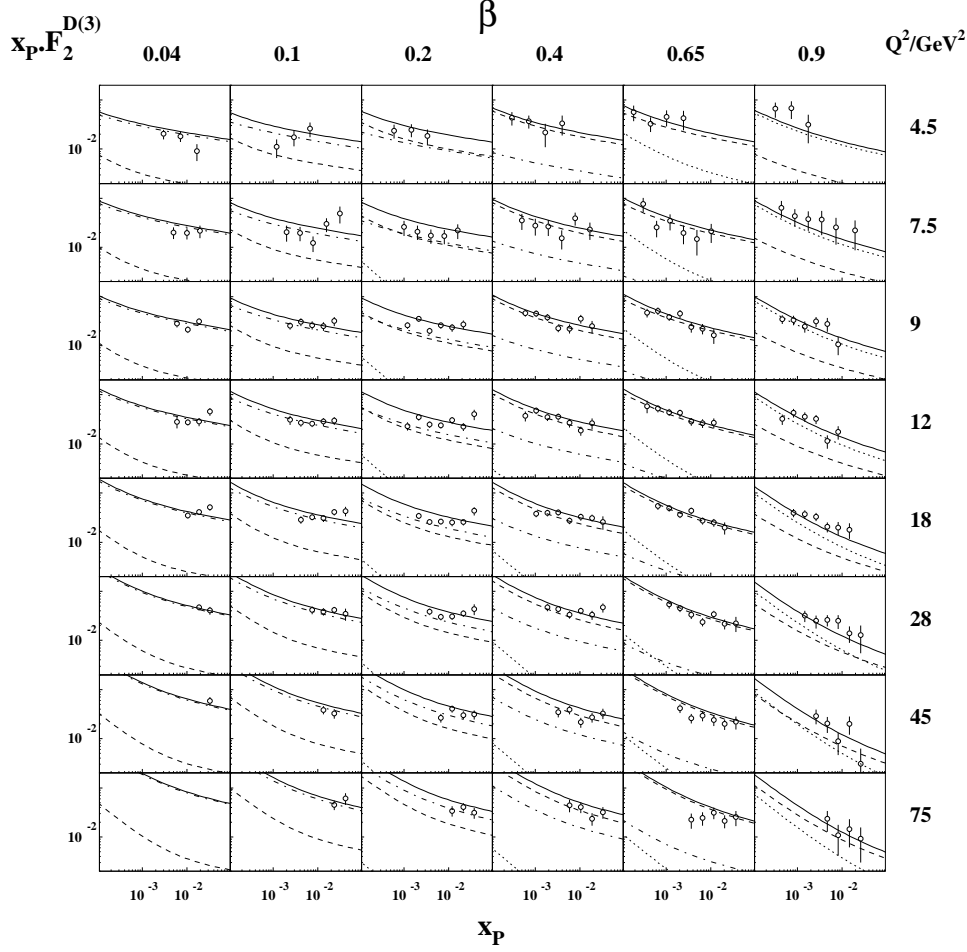


Figure 3. Contributions to $x_P F_2^{D(3)}$ compared with H1 1994 data. Full, dotted, dashed and dot dashed lines are the total, longitudinal $q\bar{q}$, transverse $q\bar{q}$ and $q\bar{q}g$ contributions respectively.

5. Acknowledgements

GRK would like to thank PPARC for a Studentship. This work was supported in part by the EU Fourth Programme ‘Training and Mobility of Researchers’, Network ‘Quantum Chromodynamics and the Deep Structure of Elementary Particles’, contract FMRX-CT98-0194 (DG 12-MIHT).

REFERENCES

1. N.N. Nikolaev and B.G. Zakharov, Z. Phys. C49 (1991) 607
2. N.N. Nikolaev and B.G. Zakharov, Z. Phys. C53 (1992) 331
3. J.R. Forshaw, G. Kerley and G. Shaw, Phys. Rev. D60 (1999) 074012, hep-ph/9903341
4. H.G. Dosch, T. Gousset, G. Kulzinger and H.J. Pirner, Phys. Rev. D55 (1997) 2602,

hep-ph/9608203

5. M. Wüsthoff, Phys. Rev. D56 (1997) 4311, hep-ph/9702201
6. K. Golec-Biernat and M. Wüsthoff, Phys. Rev. D60 (1999) 114023, hep-ph/9903358
7. J. Breitweg et al, ZEUS Collab., Eur. Phys. J. C1 (1998) 81, hep-ex/9709021
8. C. Adloff et al., H1 Collab., Zeit. Phys. C76 (1997) 613, hep-ex/9708016
9. J. Breitweg et al., ZEUS Collab., Eur. Phys. J. C6 (1999) 43, hep-ex/9807010
10. K. Golec-Biernat and M. Wüsthoff, Phys. Rev. D59 (1999) 014017, hep-ph/9807513